TISSUE ENGINEERING: Part A
Volume 17, Numbers 23 and 24, 2011

DOI: 10.1089/ten.tea.2011.0158

Expansion on Extracellular Matrix Deposited by Human Bone Marrow Stromal Cells Facilitates Stem Cell Proliferation and Tissue-Specific Lineage Potential

Ming Pei, M.D., Ph.D., Fan He, Ph.D., and Vincent L. Kish, ASEE

Our objective was to assess the rejuvenation effect of extracellular matrix (ECM) deposited by human bone marrow stromal cells (hBMSCs) on hBMSC expansion and tissue-specific lineage differentiation potential. Passage 5 hBMSCs were expanded on ECM or conventional plastic flasks (Plastic) for one passage. Cell number was counted and immunophenotype profiles were assessed using flow cytometry. Selected integrins and proliferation-related pathway signals were assessed using Western blot. The expanded cells were evaluated for their chondrogenic potential in a pellet culture system with TGF-β3-containing chondrogenic medium using gross morphology, histology, immunostaining, biochemical analysis, real-time polymerase chain reaction, Western blot, and biomechanical testing. ECM-expanded hBMSCs were further evaluated for their osteogenic potential using Alizarin Red S staining and alkaline phosphatase activity assay and for their adipogenic potential using Oil Red O staining. ECM-expanded hBMSCs exhibited an enhanced proliferation capacity and an acquired robust chondrogenic potential compared to those grown on Plastic. ECM expansion decreased intracellular reactive oxygen species and increased stage-specific embryonic antigen-4 expression in hBMSCs. ECM expansion also upregulated integrins α2 and β5 and induced a sustained activation of Erk1/2 and cyclin D1. Interestingly, upregulation of TGF-β receptor II during cell expansion and chondrogenic induction might be responsible for an enhanced chondrogenic potential in ECM-expanded hBMSCs. We also found that ECM-expanded hBMSCs had an increased osteogenic potential and decreased adipogenic capacity. ECM deposited by hBMSCs may be a promising approach to expand BMSCs from elderly patients for the treatment of large-scale bone defects through endochondral bone formation.

Introduction

Adult stem cells are considered a promising source for cell therapy and regenerative medicine, not only because they can be isolated from various adult tissues, but also because they have excellent self-renewal potential and multilineage differentiation capacities.[1,2] The current expansion technique *in vitro*, however, limits the utilization of adult stem cells due to inadequate cell quantity and impaired multilineage differentiation potential after monolayer culture.[3,4] We recently developed a novel adult stem cell expansion system based on the three-dimensional (3D) extracellular matrix (ECM) deposited by porcine synovium-derived stem cells (pSDSCs). This system dramatically improved the proliferation and chondrogenic capacity of expanded pSDSCs.[4,5] This 3D ECM is proposed to mimic the *in vivo* microenvironment, thus directing stem cells in morphology, cell–cell and cell–matrix interaction, self-renewal, and differentiation.[3–6] Compared to conventional two-dimensional (2D) reconstituted matrices, which are usually coated with a matrix protein such as fibronectin,[7] collagen I,[8] or laminin,[9] the native cell-deposited ECM not only provides 3D structure but also possesses complex components to affect the cell signaling pathway.[3,4,10]

A recent study reported that ECM made from mouse bone marrow stromal cells (mBMSCs) facilitates expansion of marrow-derived mesenchymal progenitor cells and prevents their differentiation into osteoblasts.[3] They demonstrated that ECM expansion enhanced mBMSC osteogenic and adipogenic capacities. However, there was no study investigating whether ECM deposited by BMSCs could enhance expanded BMSC chondrogenic potential. We also wondered whether the ECM rejuvenation effect also worked for human BMSCs (hBMSCs), which is a critical step for future clinical application. Moreover, the potential mechanisms underlying ECM rejuvenation need to be elucidated. In this study, we expanded hBMSCs on ECM deposited by hBMSCs or conventional plastic flasks for one passage. ECM-expanded

Stem Cell and Tissue Engineering Laboratory, Division of Exercise Physiology, Department of Orthopaedics, West Virginia University, Morgantown, West Virginia.

hBMSCs were evaluated for cell proliferation and related signaling pathways as well as immunophenotype profile changes. ECM-expanded hBMSCs were also isolated and assessed for their multilineage differentiation capacities.

Materials and Methods

Preparation of decellularized ECM deposited by hBMSCs

hBMSCs were purchased from Lonza Group Ltd. (Basel, Switzerland). Conventional plastic flasks were pretreated with a 0.2% gelatin solution (Sigma, St. Louis, MO) at 37°C for 1 h, sequentially followed by 1% glutaraldehyde (Sigma) and 1 M ethanolamine (Sigma) for 30 min. hBMSCs pooled from five donors (20–43 years old, average 25 years old; three males and two females) were seeded on pretreated flasks at a density of 3000 cells/cm^2 in growth medium (α-MEM [Invitrogen, Carlsbad, CA] containing 10% fetal bovine serum, 100 U/mL penicillin, 100 μg/mL streptomycin, and 0.25 μg/mL fungizone) for 7 days. After reaching 90% confluence, 50 μg/mL of L-ascorbic acid phosphate (Wako, Richmond, VA) was added and culture was continued for an additional 8 days. To remove embedded cells, ECM deposited by hBMSCs was incubated with 0.5% Triton X-100 containing 20 mM ammonium hydroxide at 37°C for 5 min, followed by 100 U/mL DNase I at 37°C for 1 h and stored at 4°C.

In vitro *expansion of hBMSCs on plastic and ECM*

Passage 5 hBMSCs were expanded on two different substrates: conventional plastic flasks (Plastic) or flasks coated with hBMSC-derived ECM. Nonadherent cells were removed by medium change every 3 days. Cell number was calculated by a counting hemocytometer (Hausser Scientific, Horsham, PA).

Measurement of intracellular reactive oxygen species

Intracellular reactive oxygen species (ROS) generation was measured with 2′,7′-dichlorofluorescein diacetate (DCF-DA; Sigma). In brief, 2×10^5 of cells ($n=3$) were incubated with 10 μM of DCF-DA at 37°C for 10 min. After rinsing twice with phosphate-buffered saline (PBS), DCF fluorescence was measured by a BD dual laser FACS Calibur (BD Biosciences, San Jose, CA) using the FCS Express software package (De Novo Software, Los Angeles, CA); 10,000 events of each sample were analyzed.

Flow cytometry analysis

The following primary antibodies were used in flow cytometry to detect hBMSC surface immunophenotype profiles: CD14, CD24, integrin β1 (CD29), CD44, CD45, CD71, CD73, and CD166 were purchased from Abcam (Cambridge, MA); CD105, the stage-specific embryonic antigen-4 (SSEA-4), integrins of α1 (CD49a), α2 (CD49b), α3 (CD49c), α4 (CD49d), α5 (CD49e), α6 (CD49f), β3 (CD61), and β4 (CD104) were from Santa Cruz Biotechnology (Santa Cruz, CA); CD90 was from BD Pharmingen (BD Biosciences); and integrin β5 was from Cell Signaling Technology (Danvers, MA). The isotype controls IgG1 and IgG2a (Beckman Coulter, Fullerton, CA) were used and the secondary antibody was goat anti-mouse IgG (H + L) R-phycoerythrin conjugated (Invitrogen). Samples ($n=3$) of each 0.2×10^6 expanded cells were incubated on ice in cold PBS containing 0.1% ChromPure Human IgG whole molecule (Jackson ImmunoResearch Laboratories, West Grove, PA) and 1% NaN_3 (Sigma) for 30 min. Then, the cells were sequentially incubated in the dark in the primary and secondary antibodies for 30 min. The fluorescence was analyzed by a FACS Calibur (BD Biosciences) using FCS Express software package (De Novo Software).

Chondrogenic differentiation of hBMSCs

Three hundred thousand expanded hBMSCs were centrifuged to form pellets in 15-mL polypropylene tubes at 500 *g* for 5 min. After 24 h incubation, the pellets were cultured in a serum-free chondrogenic medium (high-glucose DMEM, 40 μg/mL proline, 100 nM dexamethasone [Sigma], 100 U/mL penicillin, 100 μg/mL streptomycin, 0.1 mM L-ascorbic acid-phosphate, and ITS™ Premix [BD Biosciences] with the supplementation of 10 ng/mL of TGF-β3 [PeproTech, Inc., Rocky Hill, NJ]). The pellets at days 0, 7, and 15 were collected for further analysis.

Histology and immunohistochemistry

The pellets ($n=2$) were fixed in 4% paraformaldehyde, embedded in paraffin blocks, and cut into 5-μm-thick sections. Alcian blue (Sigma) staining was used to detect sulfated glycosaminoglycans (GAGs). Immunohistochemistry was used to detect collagens I, II, and X. Briefly, the sections were incubated with primary antibodies against collagen I (Sigma), collagen II (II-II6B3, Developmental Studies Hybridoma Bank [DSHB], Iowa City, IA), and collagen X (Sigma), followed by the secondary antibody of biotinylated horse anti-mouse IgG (Vector, Burlingame, CA), and detected by using Vectastain ABC reagent (Vector) with 3,3′-diaminobenzidine as a substrate.

Biochemical analysis

The representative pellets ($n=4$) were digested at 60°C for 6 h with 125 μg/mL papain in PBE buffer (100 mM phosphate and 10 mM EDTA, pH 6.5) containing 10 mM cysteine. DNA amount was measured using Quant-iT™ PicoGreen® dsDNA assay kit (Invitrogen) with a CytoFluor® Series 4000 (Applied Biosystems, Foster City, CA). GAG amount was measured using dimethylmethylene blue dye and a Spectronic™ BioMate™ 3 Spectrophotometer (Thermo Scientific, Milford, MA) with bovine chondroitin sulfate (Sigma) as a standard.

Western blot

Radioimmunoprecipitation assay lysis buffer supplemented with halt protease and phosphatase inhibitor cocktail (Thermo Scientific) was used to extract protein from hBMSCs. The samples were denatured and separated by NuPAGE® Novex® Bis–Tris Mini Gels (Invitrogen) at 200 V for 45 min at 4°C, and then transferred onto a nitrocellulose membrane (Invitrogen) using XCell II™ blot module (Invitrogen) at 30 V for 1 h at 4°C. The membranes were first blocked in SuperBlock (TBS) Blocking Buffer (Thermo Scientific), and then incubated with the primary monoclonal antibodies at the recommended dilution at 4°C overnight. The membranes were incubated in the secondary antibody of

goat anti-mouse IgG (H + L) or goat anti-rabbit IgG (H + L) (Thermo Scientific) for 40 min. The exposure used SuperSignal® West Pico Chemiluminescent Substrate (Thermo Scientific) and CL-XPosure™ Film (Thermo Scientific). The following primary antibodies were used in immunoblotting: integrin α2, integrin α5, cyclin D1, TGF-β receptor II (TGF-β RII), and phospho-TGF-β RII (Tyr 424) were purchased from Santa Cruz Biotechnology; integrin β5, phospho-cyclin D1 (Thr286), phospho-p44/42 MAPK [extracellular-signal regulated kinases 1/2 (Erk1/2)] (Thr202/Tyr204), and p44/42 MAPK (Erk1/2) were from Cell Signaling Technology; Sox9 and β-actin were from Abcam; and collagen II (CIIC1) was from DSHB.

Biomechanical testing

The representative pellets ($n = 4$) were placed into a reservoir filled with PBS and loaded onto the custom miniature stepper motor-driven compression device. This device used a 10 g load and a miniature displacement readout. A small preload of 10^{-4} N was applied before a 10% strain at 1 s duration. From the linear portion of the load displacement curve, the stiffness and Young's modulus were calculated for the spherical pellet according to a previous report.[11]

Real-time polymerase chain reaction

The total RNA from pellets ($n = 4$) was extracted using TRIzol® (Invitrogen). One microgram mRNA was used for reverse transcriptase (RT) with the High-Capacity cDNA Archive Kit at 37°C for 120 min as recommended by the manufacturer (Applied Biosystems). Chondrogenic marker genes [*collagen I* (Assay ID Hs00164004_m1), *collagen II* (Assay ID Hs00156568_m1), and *collagen X* (Assay ID Hs00166657_m1)] were customized by Applied Biosystems as part of the Custom TaqMan® Gene Expression Assays. Eukaryotic 18S rRNA (Assay ID HS99999901_s1) was carried out as the endogenous control gene. Real-time polymerase chain reaction (PCR) was performed with the iCycler iQ™ Multi Color RT-PCR Detection and calculated by computer software (Perkin-Elmer, Waltham, MA). Relative transcript levels were calculated as $\chi = 2^{-\Delta\Delta Ct}$, in which $\Delta\Delta Ct = \Delta E - \Delta C$, $\Delta E = Ct_{exp} - Ct_{18s}$, and $\Delta C = Ct_{ct1} - Ct_{18s}$.

Alkaline phosphatase assay for osteogenesis

Expanded hBMSCs ($n = 3$) cultured for 14 days in osteogenic medium (growth medium supplemented with 0.1 μM dexamethasone, 10 mM β-glycerol phosphate, 50 μM ascorbate-2-phosphate, and 0.01 μM 1,25-dihydroxyvitamin D3) were collected for alkaline phosphatase (ALP) activity assay with a reagent kit (Sigma) by measuring the formation of *p*-nitrophenol (*p*-NP) from *p*-nitrophenyl phosphate following the manufacturer's instructions. Cell cultures were lysed in a buffer containing 1.5 M Tris–HCl, 1 mM $ZnCl_2$, and 1 mM $MgCl_2$, pH 9.0, containing 2% Triton X-100, and reacted with phosphatase substrate reagent (2 mg/mL) in a microplate. *p*-NP was quantified based on the spectrophotometric absorbance at 405 nm, and enzymatic activity was expressed as millimoles of *p*-NP/min/μg DNA.

Accumulated calcium assay for osteogenesis

Expanded hBMSCs ($n = 3$) cultured for 14 days in osteogenic medium were fixed with 70% ice-cold ethanol for 1 h, and then incubated in 40 mM Alizarin Red S (ARS) at pH 4.2 for 20 min at room temperature with agitation on an orbital shaker (60 rpm). After two intensive rinses with deionized water, matrix mineral-bound staining was photographed under a Nikon TE300 phase-contrast microscope (Nikon, Tokyo, Japan). Quantification of staining was performed by incubating cells with a solution of 10% acetic acid and 20% methanol to extract the calcium-chelated Alizarin Red stain for 15 min. Samples were analyzed for absorption at 450 nm, which was normalized to total DNA amount for standardization.

Intracellular lipid-filled droplet formation assays for adipogenesis

Expanded hBMSCs cultured for 14 days in adipogenic medium [growth medium supplemented with 1 μM dexamethasone, 0.5 mM isobutyl-1-methyxanthine, 200 μM indomethacin, and 10 μM insulin]. The cultures ($n = 3$) were fixed in 4% paraformaldehyde and stained with a 0.6% (w/v) Oil Red O (ORO) solution (60% isopropanol, 40% water) for 15 min. Intracellular lipid-filled droplet-bound staining was photographed under a Nikon TE300 phase-contrast microscope (Nikon). Quantification of staining was performed by incubating cells with 1 mL of isopropyl alcohol for 5 min to extract the intracellular lipid-filled droplet-bound ORO stain. A 200-mL extract was placed in a transparent 96-well flat-bottom culture plate and the absorbance of the extract was measured using a spectrophotometer at 510 nm. Absorption values were normalized to total DNA amount for standardization.

Statistical analysis

Statistics were assessed by one-way analysis of variance; *p*-values less than 0.05 were considered statistically significant.

Results

ECM expansion promoted hBMSC proliferation

hBMSCs grown on Plastic appeared large and flattened; in contrast, hBMSCs expanded on ECM were smaller with a spindle-like shape. Upon reaching confluence, the cells overlapped. Interestingly, hBMSCs grown on ECM underwent directional migration along the ECM fibrils, whereas the cells expanded on Plastic showed random orientation (Fig. 1A). After 7-day expansion, hBMSCs on ECM yielded 16.8 ± 2.3-fold increase of the cell number compared to 6.7 ± 0.4-fold increase in the Plastic group (Fig. 1B).

To determine whether ECM promoting hBMSC expansion has any relationship with cell stress and/or maintenance of stem cell stemness, we examined the intracellular ROS (staining with DCF-DA) and SSEA-4 expression in hBMSCs expanded on Plastic and ECM using flow cytometry. Compared to the initial mean fluorescence intensity (MFI) of DCF as 184 ± 15, the 4-day-expansion on Plastic yielded 202 ± 5, which was 2.1-fold that on ECM (98 ± 12); 7-day-expansion on Plastic yielded 241 ± 15, which was 1.7-fold that on ECM (139 ± 5; Fig. 1C). The above data suggested that hBMSCs expanded on Plastic showed a markedly higher level of DCF fluorescence compared with those grown on ECM. Our data also indicated that SSEA-4 expression in hBMSCs was

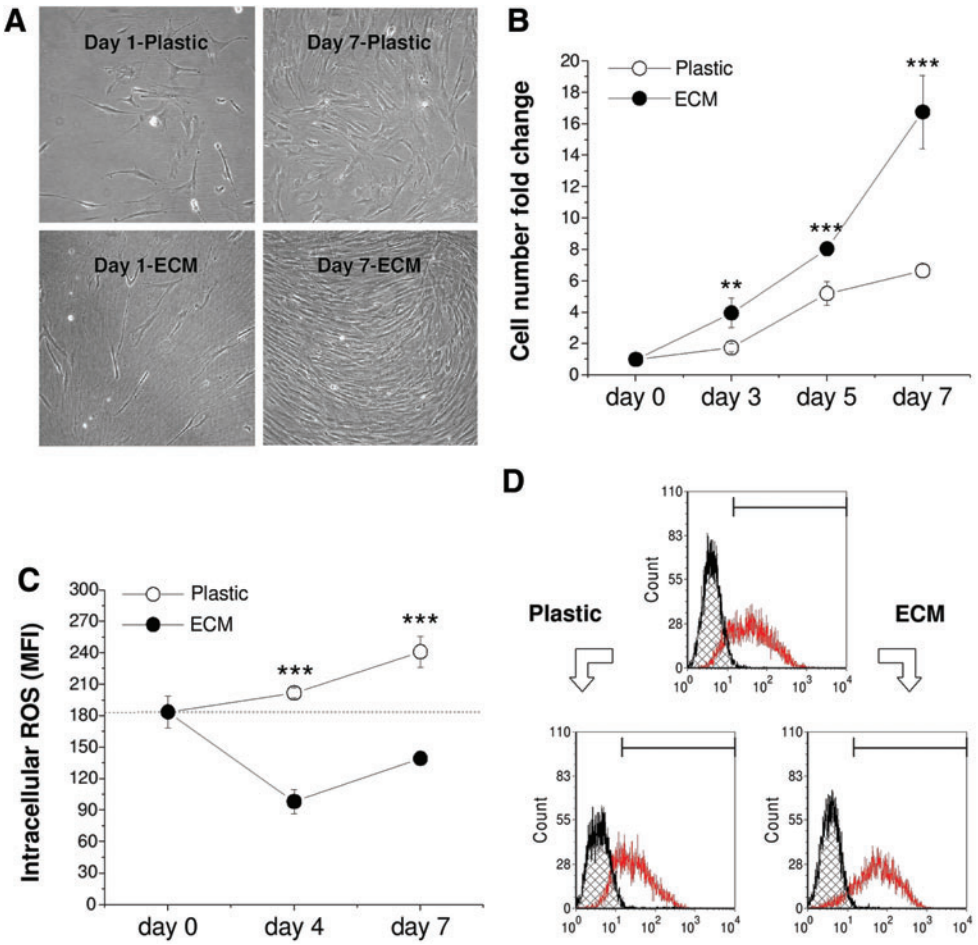

FIG. 1. One passage expansion on extracellular matrix (ECM) resulted in significant changes of cell morphology **(A)**, cell number **(B)**, intracellular reactive oxygen species (ROS) level **(C)**, and stage-specific embryonic antigen-4 expression **(D)**. **(C)** and **(D)** were measured using flow cytometry. Significant differences compared to corresponding group were indicated as follows: $^{**}p < 0.01$; and $^{***}p < 0.001$. Data were shown as average ± SD for $n = 4$. Color images available online at www.liebertonline.com/tea

upregulated during ECM expansion but downregulated during Plastic expansion (Percentage: 84.8 on ECM and 66.5 on Plastic compared to 75.2 before expansion, and MFI: 100 on ECM and 47.8 on Plastic compared to 71.9 before expansion; Fig. 1D).

To determine the effect of ECM expansion on hBMSC immunophenotype profiles, flow cytometry was used to identify the expression of integrin markers [integrins α1 (CD49a), α2 (CD49b), α3 (CD49c), α4 (CD49d), α5 (CD49e), α6 (CD49f), β1 (CD29), β3 (CD61), β4 (CD104), and β5], adhesion molecules (CD24, CD106, CD166), mesenchymal stem cell markers (CD44, CD71, CD73, CD90, CD105), and hematopoietic stem cell markers (CD14, CD45) during cell expansion (Fig. 2A, B). Four-surface antigen expression level (MFI) increased in hBMSCs expanded on ECM compared to those grown on Plastic: integrin α2 (40 vs. 15), integrin α4 (15 vs. 12), CD71 (12 vs. 9), and integrin β5 (374 vs. 74). Ten-antigen expression level decreased after hBMSCs were expanded on ECM compared to on Plastic: integrin β1 (141 vs. 210), integrin α1 (12 vs. 22), integrin α3 (227 vs. 695), integrin α5 (68 vs. 103), integrin β3 (14 vs. 19), CD90 (367 vs. 502), CD105 (177 vs. 273), and CD166 (58 vs. 66). However, the seven-antigen expression level (CD14, CD24, CD44, CD45, integrin α6, CD73, and integrin β4) showed no difference in hBMSCs after expansion on ECM and Plastic.

To confirm that ECM expansion induced a dramatic change in selected integrins and explore whether ECM expansion upregulated a proliferation-related pathway, Western blot was used to quantify expression levels of integrins α2, α5, and β5, cyclin D1, and Erk1/2 (Fig. 3). Our data demonstrated that ECM expansion yielded hBMSCs with upregulation of integrins α2 and β5 and downregulation of integrin α5, consistent with our flow cytometry data. To illuminate the potential mechanism underlying ECM enhancing hBMSC expansion, we used antibodies to probe the steady-level and phosphorylation of cyclin D1 and Erk1/2. We found a higher expression and phosphorylation of cyclin D1 and Erk1/2 in hBMSCs expanded on ECM compared to those grown on Plastic, suggesting that ECM expansion might be responsible for the improved hBMSC proliferation through cyclin D1 and Erk1/2.

ECM expansion enhanced hBMSC chondrogenic potential

After a 15-day chondrogenic induction, pellets from ECM-expanded hBMSCs exhibited a larger size than those grown on Plastic. To determine whether the pellets were premature cartilage tissue, histology and immunostaining were used to detect chondrogenic markers. Despite there being no positive staining in either group at day 0 (not shown here), 15-day-pellets were intensively stained by sulfated GAGs, and collagens I and II in the ECM group compared to minimal staining of GAGs and collagen I and nondetectable staining

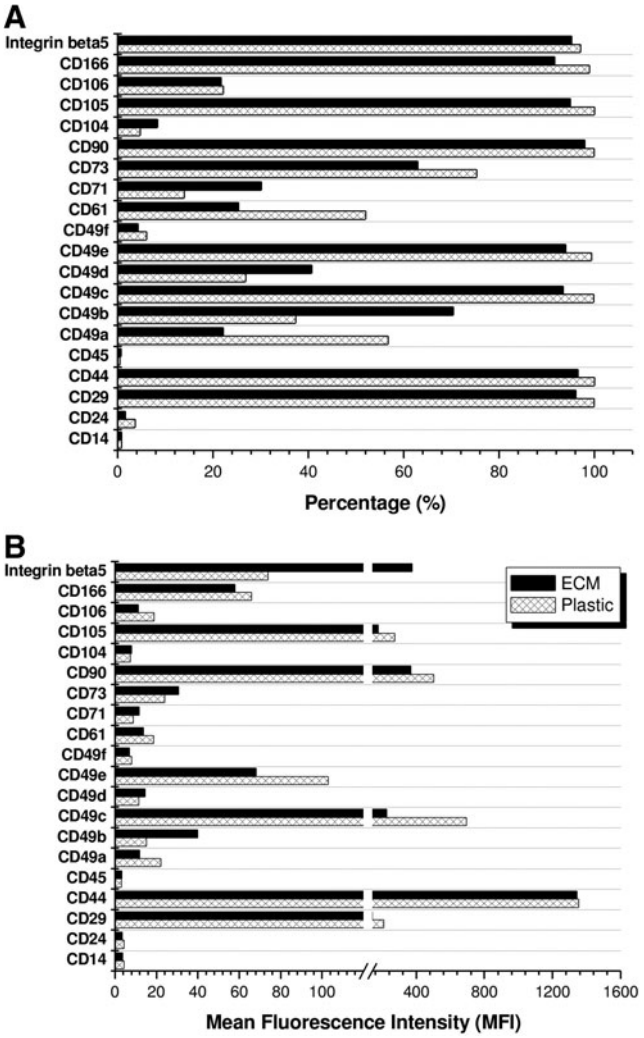

FIG. 2. One passage expansion on ECM resulted in significant changes of immunophenotype profiles of human bone marrow stromal cells (hBMSCs) in percentage **(A)** and MFI **(B)**. The measured surface phenotypes consisted of integrin markers (integrins α1 [CD49a], α2 [CD49b], α3 [CD49c], α4 [CD49d], α5 [CD49e], α6 [CD49f], β1 [CD29], β3 [CD61], β4 [CD104], and β5), adhesion molecules (CD24, CD106, CD166), mesenchymal stem cell markers (CD44, CD71, CD73, CD90, CD105), and hematopoietic stem cell markers (CD14, CD45).

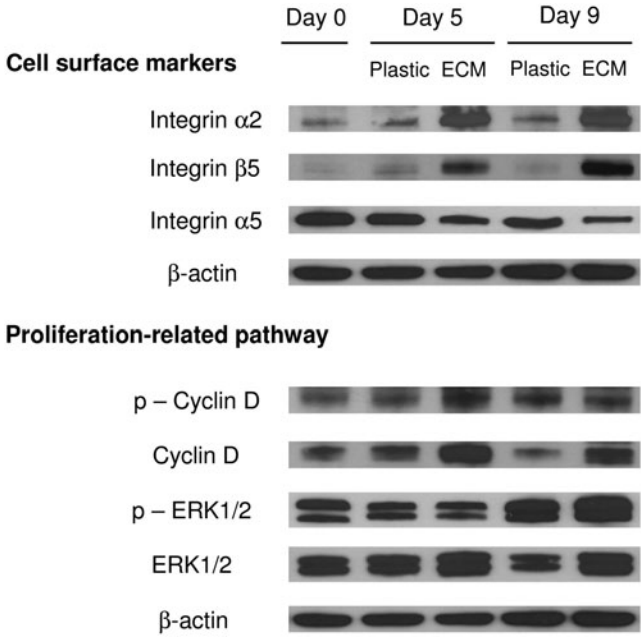

FIG. 3. Western blot was used to evaluate selected cell surface integrin (α2, α5, and β5) expression and proliferation-related signaling pathway [phospho-cyclin D1 (Thr286), cyclin D1, phospho-p44/42 MAPK (Erk1/2) (Thr202/Tyr204), and p44/42 MAPK (Erk1/2)] in expanded hBMSCs. β-actin was used as an internal control for protein loading.

of collagen II in the Plastic group. Collagen X was nearly negative in both pellets (Fig. 4A). To determine whether TGF-β receptors in hBMSCs were modulated by ECM expansion, TGF-β RI and RII were assessed using Western blot. Compared to the same tendency of TGF-β RI in both groups (not shown here), ECM-expanded hBMSCs exhibited a higher expression of phospho-TGF-β RII (especially at day 7) than those grown on Plastic (Fig. 4B), which probably was related with a higher level of TGF-β RII in hBMSCs resulting from ECM expansion (Fig. 4C). Our data suggested that a serum-free TGF-β-containing chondrogenic medium might upregulate phospho-TGF-β RII expression, which was responsible for the upregulation of chondrogenic markers, Sox9 and collagen II, in ECM-expanded hBMSCs (Fig. 4B). To assess functional properties of ECM-expanded hBMSCs, 15-day pellets were used to examine stiffness and Young's modulus. Pellets from ECM-expanded hBMSCs exhibited 39.9 ± 9.5 N/M in stiffness compared to 24.9 ± 4.7 N/M in the Plastic group (Fig. 4D). In addition, pellets from ECM-expanded hBMSCs exhibited 0.6 ± 0.1 MPa in Young's modulus compared to 0.3 ± 0.1 MPa in the Plastic group (Fig. 4E).

Our biochemical analysis data (Fig. 5A) indicated that ECM-expanded hBMSCs exhibited better cell viability than those grown on Plastic ($79.0\% \pm 13.7\%$ vs. $61.1\% \pm 9.5\%$, $p < 0.05$, at day 15) in a pellet culture system. Moreover, ECM-expanded hBMSCs formed pellets with a higher GAG amount and ratio of GAG to DNA (chondrogenic index) than those from Plastic expansion at either day 7 ($p < 0.01$) or day 15 ($p < 0.001$) after incubation in a serum-free chondrogenic medium. Our real-time PCR data (Fig. 5B) suggested that ECM expansion could decrease *collagen I* mRNA level (an early marker in chondrogenic differentiation) in hBMSCs; once chondrogenically induced, expanded hBMSCs in the pellet exhibited a burst at day 7 and a drop at day 15 in *collagen I* mRNA. In contrast, chondrogenic marker gene (*collagen II*) and hypertrophic marker gene (*collagen X*) continued to be upregulated in both groups; of them, ECM-expanded hBMSCs displayed a higher chondrogenic potential than those grown on Plastic ($p < 0.001$) after both 7- and 15-day chondrogenic induction.

ECM expansion enhanced osteogenic potential but decreased adipogenic capacity in hBMSCs

To determine whether ECM expansion enhanced hBMSC osteogenic and adipogenic capacities, expanded hBMSCs were isolated from either ECM or Plastic and re-plated on

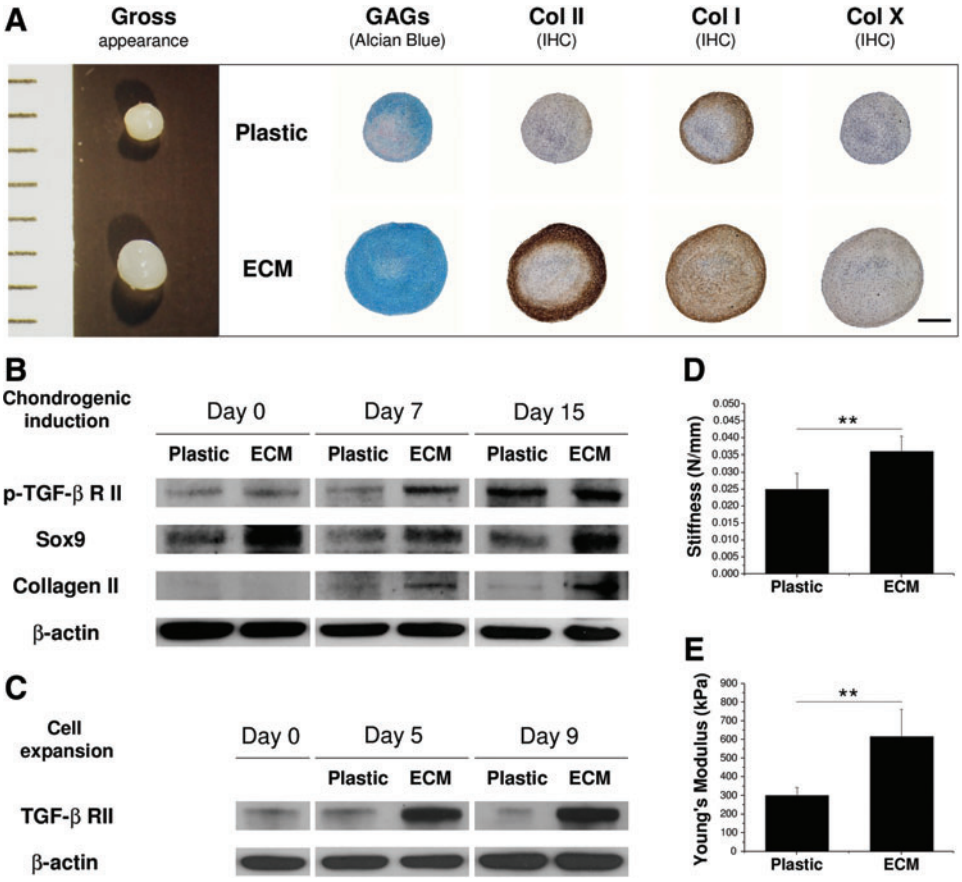

FIG. 4. Morphologic, molecular, and functional methods were used to evaluate chondrogenic potential of ECM or Plastic expanded hBMSCs in a pellet culture system after a 15-day serum-free chondrogenic induction. **(A)** Gross appearance (mm), Alcian blue staining for sulfated glycosaminoglycans (GAGs), and immunohistochemistry for collagens I, II, and X; scale bar is 800 μm; **(B, C)** Western blot was used to evaluate TGF-β RII and phospho-TGF-β RII expression during ECM expansion and subsequent chondrogenic induction in hBMSCs. Chondrogenic markers (collagen II and Sox9) were also evaluated in hBMSC chondrogenic differentiation. β-actin was used as an internal control for protein loading, and **(D, E)** biomechanical testing for stiffness (N/mm) and Young's modulus (kPa). $^{**}p < 0.01$. Data were shown as average ± SD for $n = 4$. Color images available online at www.liebertonline.com/tea

Plastic. Our data suggested that, after incubation in osteogenic medium, there was more bone nodule formation (Fig. 6A) and denser ALP staining (Fig. 6B) in ECM-expanded hBMSCs compared to those grown on Plastic. An osteogenic staining trend was also confirmed by quantification data, in which both ARS staining and ALP activity indicated that ECM-expanded hBMSCs exhibited a higher osteogenic potential than the Plastic group ($p < 0.001$). Our data (Fig. 6C) also indicated that, after incubation in adipogenic medium, large lipid droplets were evident in hBMSCs expanded on Plastic instead of on ECM. Quantitative ORO assay indicated that Plastic expanded hBMSCs displayed a higher adipogenic capacity than those grown on ECM ($p < 0.001$).

Discussion

The aim of this study was to investigate whether ECM deposited by hBMSCs could enhance Passage 5 (replicative senescent) hBMSC expansion and tissue-specific lineage capacity and explore the potential underlying mechanisms. We found that ECM deposited by hBMSCs dramatically increased hBMSC expansion. ECM-expanded hBMSCs exhibited a decreased level of intracellular ROS and an increased expression of SSEA-4. ECM-expanded hBMSCs also exhibited an upregulation of integrins α2 and β5, Erk1/2, and cyclin D1. Remarkably, ECM-expanded hBMSCs displayed an enhanced chondrogenic potential, which was demonstrated in a pellet culture system with superior cartilage structure, function, and molecular properties. This might result from an upregulation of TGF-β RII in ECM-expanded hBMSCs. Intriguingly, ECM-expanded hBMSCs exhibited an enhanced osteogenic potential but a decreased adipogenic capacity.

Cell-derived 3D ECM was recently reported to induce sustained activation of Erk1/2.[6] Erk activity stimulates cyclin D1 expression.[12] Cyclin D1 is most closely linked to cell-cycle progression through the G1 phase and the commitment of cells to enter the S phase. Cyclin D1 is termed "a sensor of the mitogenic microenvironment" because its expression is induced by many mitogen factors, including growth factors, cytokines, and hormones.[13] The continued cyclin D1 expression in the presence of mitogen requires the sustained activation of Erk.[14,15] Our study suggested that ECM-expanded hBMSCs exhibited an enhanced expression of Erk1/2 and cyclin D1 accounting for enhanced proliferation of ECM-expanded hBMSCs.

Enhanced proliferation in ECM-expanded hBMSCs may also be associated with a decreased level of intracellular ROS and an increased expression of SSEA-4. Intracellular ROS plays an important role in cell adhesion, migration, and proliferation and thus is essential for cell survival.[16] A low concentration of ROS has a promotional effect on cell adhesion,[17] whereas a high level of ROS has an inhibitory influence on cell proliferation by arresting cell cycle at the G1, S, and G2 phases through downregulation of cyclin D1 and D3 signaling.[18] Our study demonstrated that ECM could attenuate ROS level in expanded cells, which benefited cell adhesion and survival.[19] Compared to downregulation of ROS level, ECM-expanded hBMSCs exhibited upregulation of SSEA-4. SSEA-4 was originally discovered in embryonic

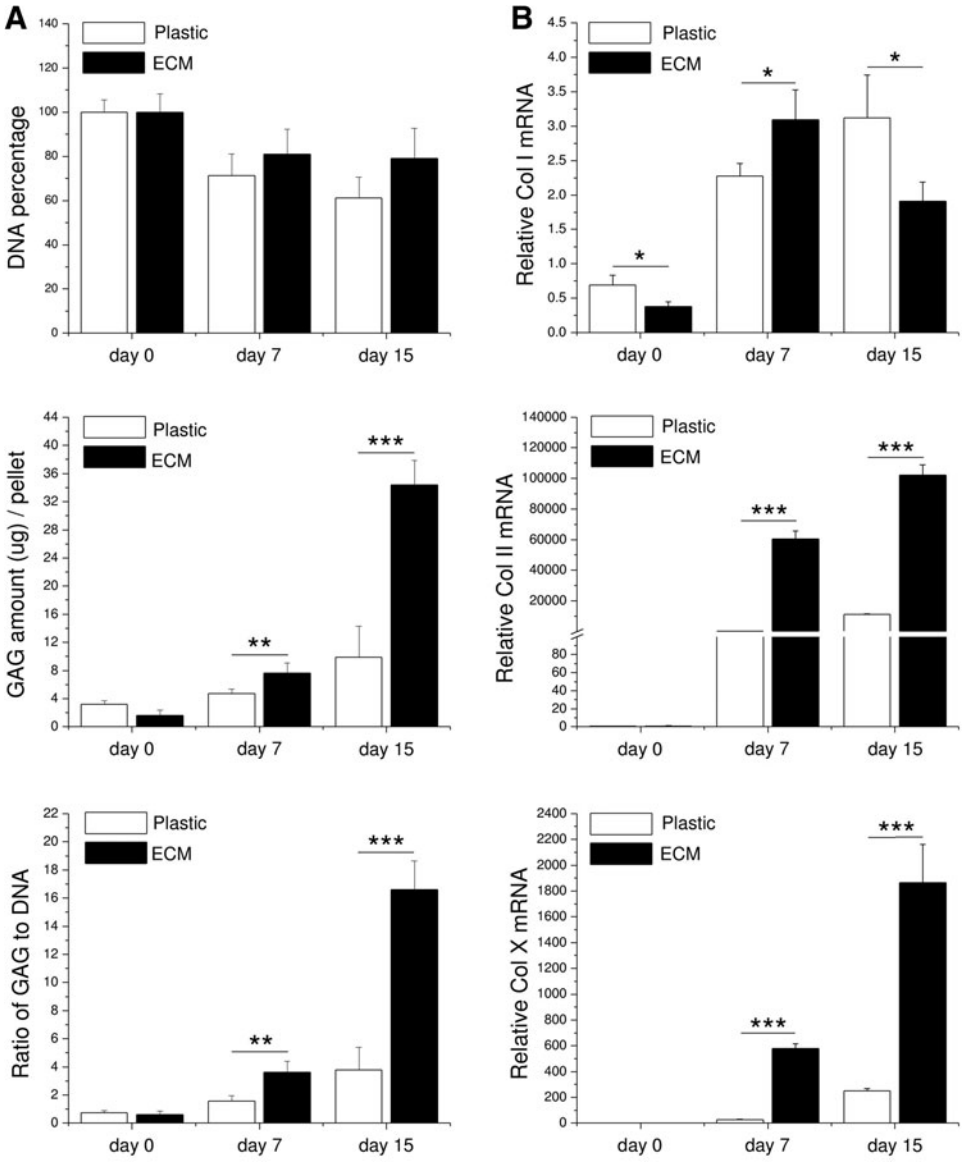

FIG. 5. Biochemistry **(A)** and real-time PCR **(B)** were used to evaluate chondrogenic differentiation of expanded hBMSCs on either ECM or Plastic in a pellet culture system after a 15-day serum-free chondrogenic induction. Ratio of GAG to DNA was referred to as chondrogenic index. Chondrogenic marker genes, *collagens I, II,* and *X*, were quantified at the mRNA level. All 18S rRNA normalized genes were shown as a ratio to the value of day 0 pellet cells from Plastic expansion. Significant differences were indicated as follows: $*p < 0.05$; $**p < 0.01$; and $***p < 0.001$. Data were shown as average ± SD for $n = 4$.

stem cells and was recently reported to express in BMSCs.[20] Growth kinetic analysis revealed that assorted SSEA-4-positive BMSCs could be grown for more than 7 weeks without senescence,[20] indicating that the upregulation of SSEA-4 expression in this study might be directly correlated to enhanced proliferation in ECM-expanded hBMSCs.

Consistent with our recent findings,[4,5] ECM expansion not only promoted cell proliferation but also dramatically enhanced hBMSC chondrogenic potential. Interestingly, we found that TGF-β RII level in ECM-expanded hBMSCs was upregulated, whereas TGF-β RI level was comparable to that grown on Plastic (data not shown). The high expression of TGF-β RII during ECM expansion and the sustained steady-state phosphorylated level of TGF-β RII in TGF-β1-contained chondrogenic induction could be responsible for the upregulation of Sox9 and collagen II in ECM-expanded hBMSCs.[21] Moreover, decorin, fibronectin, laminins, and collagens I and III, identified in the 3D BMSC-deposited ECM,[3,19] played an important role in TGF-β receptor responsiveness and modulating TGF-β bioactivity during cell proliferation and differentiation.[22,23] The mechanism of elevated TGF-β RII expression is still unclear but possibly related to the crosstalk between TGF-β receptors and integrin.[24,25]

Interaction of cells with ECM mainly takes place via integrin receptors in virtually all cell types. Integrins are heterodimeric membrane molecules that mediate cell adhesion and signaling mechanisms.[26] The ECM plays a key role in modulating function and phenotype of the embedded cells and contains integrins as adhesion receptors mediating cell–cell and cell–matrix interactions. In our study, we found that ECM-expanded hBMSCs exhibited enhanced levels of integrins α2 and β5 and a decreased level of integrin α5. Integrin β5, also termed an osteopontin receptor, was constantly expressed in BMSCs.[27] An osteopontin receptor might be involved in the processes of cellular migration and proliferation.[28] Further, this receptor might assist in the cellular differentiation *in vitro*.[29] A recent report suggested that this receptor seems to play a role during chondrogenic differentiation; in addition, integrin α2 (the receptor for laminin and collagen) might assist the start of chondrogenic

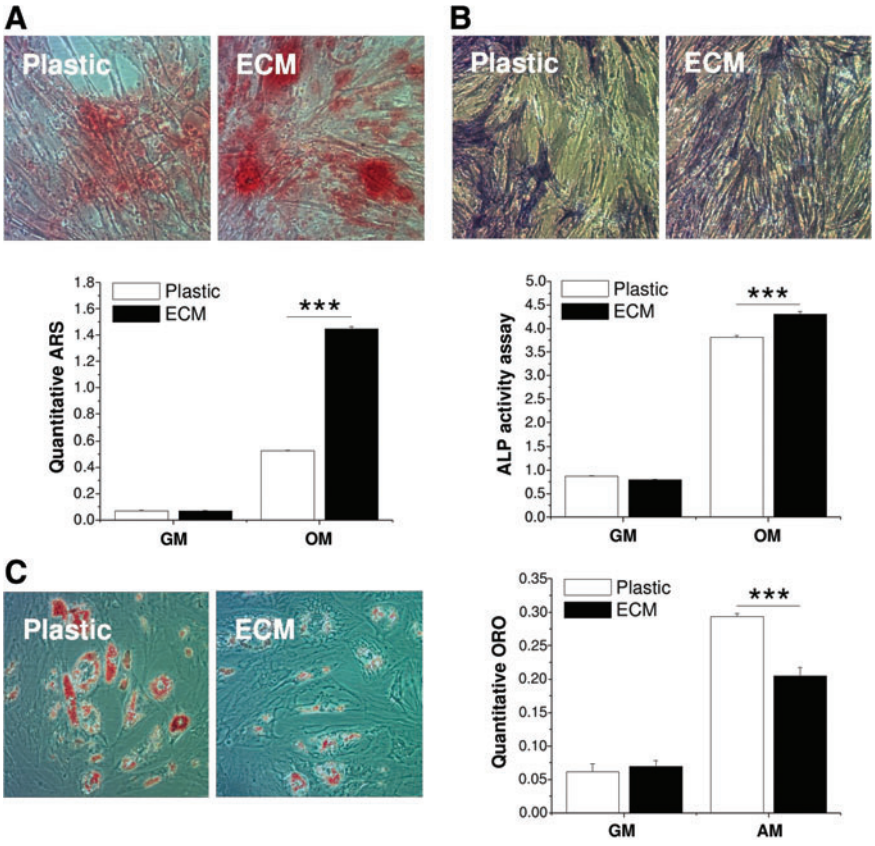

FIG. 6. ECM-expanded hBMSCs were also evaluated for their osteogenic and adipogenic capacities. After incubation in osteogenic medium (OM) or growth medium (GM) for 14 days, osteogenesis was assessed with accumulated calcium deposition stained with Alizarin Red S (ARS) **(A)** and alkaline phosphatase (ALP) **(B)** staining and activity assay. After incubation in adipogenic medium (AM) or growth medium (GM) for 14 days, adipogenesis was assessed with intracellular lipid-filled droplet formation stained with ORO and quantification **(C)**. Significant differences were indicated as follows: ***$p < 0.001$. Data were shown as average ± SD for $n = 3$. Color images available online at www.liebertonline.com/tea

differentiation.[27] Therefore, the upregulation of integrins α2 and β5 may account for enhanced chondrogenic potential in ECM-expanded hBMSCs. Integrins also played a crucial role in chondrogenesis such as integrin β_1[30] and interacted with type II collagen through integrin α_2 when differentiating to mature chondrocytes.[31] Although integrin α5β1 (the fibronectin receptor) was expressed in undifferentiated stem cells, its expression rose during chondrogenic differentiation in hBMSCs.[27] The decrease of integrin α5β1 in hBMSCs might suggest that ECM expansion could rejuvenate hBMSCs into an undifferentiated state.

Our recent study demonstrated that ECM deposited by pSDSCs not only improved pSDSC expansion but also enhanced pSDSC chondrogenic potential with decreased osteogenic and adipogenic capacities.[4] Despite the fact that ECM enhanced expanded stem cell chondrogenic potential, the current study demonstrated that ECM also enhanced hBMSC osteogenic capacity. This discrepancy might be from their unique properties as tissue-specific stem cells. There is increasing evidence demonstrating that SDSCs are a cartilage tissue-specific stem cell.[32–37] In contrast, BMSCs exhibited robust osteogenic differentiation ability, as was documented *in vitro* and *in vivo*.[2,38,39] Even incubated in a serum-free chondrogenic medium, BMSCs tend to differentiate into hypertrophic chondrocytes,[40,41] which was also shown in this study.

Consistent with a previous report,[3] ECM dramatically promoted hBMSC expansion and ECM-expanded hBMSCs displayed an enhanced osteogenic potential. However, our data also suggested that hBMSCs exhibited a decreased adipogenic capacity after expansion on ECM, despite enhanced adipogenesis in a previous study.[3] A possible reason for this discrepancy might result from the induction for multi-lineage differentiation on the different substrates. Chen *et al.* induced mBMSC expansion and differentiation on the same ECM deposited by mBMSCs.[3] In contrast, we only used ECM to expand hBMSCs; the expanded hBMSCs were then isolated and re-plated on other conventional plastic flasks for the assessment of osteogenic and adipogenic differentiation. Since decellularized stem cell matrix could enhance stem cell expansion but inhibit expanded stem cell differentiation, we chose to induce expanded stem cell differentiation in separate flasks.

In summary, our study found that utilization of 3D cell-deposited ECM in hBMSC expansion was able to dramatically increase cell proliferation, attenuate cell stress, and enhance chondrogenic potential. We also found that 3D ECM could induce sustained activation of Erk1/2 and phosphorylated cyclin D1 in expanded hBMSCs. The enhanced chondrogenic capacity in ECM-expanded hBMSCs was related to the high expression and sensitivity of TGF-β RII. Due to the complexity of 3D cell-deposited ECM, the cell signaling transduction is different from that in 2D monolayer culture and needs to be elucidated in future investigations. In addition, the cell variability needs to be determined in a comprehensive way (categorized by the age, gender, and other factors of the donor) before this approach can be applied in clinics.

Acknowledgments

The authors thank Suzanne Smith for her help in editing the article and Dr. Kathleen Brundage for her help in

performing flow cytometry and data analysis. Imaging experiments were performed in the West Virginia University Microscope Imaging Facility, which is supported in part by the Mary Babb Randolph Cancer Center and NIH grant P20 RR016440.

Disclosure Statement

No competing financial interests exist.

References

1. Liechty, K.W., MacKenzie, T.C., Shaaban, A.F., Radu, A., Moseley, A.M., Deans, R., Marshak, D.R., and Flake, A.W. Human mesenchymal stem cells engraft and demonstrate site-specific differentiation after *in utero* transplantation in sheep. Nat Med **6,** 1282, 2000.
2. Pittenger, M.F., Mackay, A.M., Beck, S.C., Jaiswal, R.K., Douglas, R., Mosca, J.D., Moorman, M.A., Simonetti, D.W., Craig, S., and Marshak, D.R. Multilineage potential of adult human mesenchymal stem cells. Science **284,** 143, 1999.
3. Chen, X., Dusevich, V., Feng, J.Q., Manolagas, S.C., and Jilka, R.L. Extracellular matrix made by bone marrow cells facilitates expansion of marrow-derived mesenchymal progenitor cells and prevents their differentiation into osteoblasts. J Bone Miner Res **22,** 1943, 2007.
4. He, F., Chen, X., and Pei, M. Reconstruction of an *in vitro* tissue-specific microenvironment to rejuvenate synovium-derived stem cells for cartilage tissue engineering. Tissue Eng Part A **15,** 3809, 2009.
5. Li, J., and Pei, M. Optimization of an *in vitro* three-dimensional microenvironment to reprogram synovium-derived stem cells for cartilage tissue engineering. Tissue Eng Part A **17,** 703, 2011.
6. Damianova, R., Stefanova, N., Cukierman, E., Momchilova, A., and Pankov, R. Three-dimensional matrix induces sustained activation of ERK1/2 via Src/Ras/Raf signaling pathway. Cell Biol Int **32,** 229, 2008.
7. Dao, M.A., Hashino, K., Kato, I., and Nolta, J.A. Adhesion to fibronectin maintains regenerative capacity during *ex vivo* culture and transduction of human hematopoietic stem and progenitor cells. Blood **92,** 4612, 1998.
8. Eslaminejad, M.B., Mirzadeh, H., Nickmahzar, A., Mohamadi, Y., and Mivehchi, H. Type I collagen gel in seeding medium improves murine mesencymal stem cell loading onto the scaffold, increases their subsequent proliferation, and enhances culture mineralization. J Biomed Mater Res B Appl Biomater **90,** 659, 2009.
9. Klees, R.F., Salasznyk, R.M., Kingsley, K., Williams, W.A., Boskey, A., and Plopper, G.E. Laminin-5 induces osteogenic gene expression in human mesenchymal stem cells through an ERK-dependent pathway. Mol Biol Cell **16,** 881, 2005.
10. Cukierman, E., Pankov, R., Stevens, D.R., and Yamada, K.M. Taking cell-matrix adhesions to the third dimension. Science **294,** 1708, 2001.
11. Rodriguez, F., Patel, S.K., and Cohen, C. Measuring the modulus of a sphere by sequeezing between parallel plates. J Appl Polymer Sci **5,** 285, 1990.
12. Roovers, K., and Assoian, R.K. Integrating the MAP kinase signal into the G1 phase cell cycle machinery. Bioessays **22,** 818, 2000.
13. Matsushime, H., Quelle, D.E., Shurtleff, S.A., Shibuya, M., Sherr, C.J., and Kato, J.Y. D-type cyclin-dependent kinase activity in mammalian cells. Mol Cell Biol **14,** 2066, 1994.
14. Villanueva, J., Yung, Y., Walker, J.L., and Assoian, R.K. ERK activity and G1 phase progression: identifying dispensable versus essential activities and primary versus secondary targets. Mol Biol Cell **18,** 1457, 2007.
15. Weber, J.D., Raben, D.M., Phillips, P.J., and Baldassare, J.J. Sustained activation of extracellular-signal-regulated kinase 1 (ERK1) is required for the continued expression of cyclin D1 in G1 phase. Biochem J **326,** 61, 1997.
16. Rollet-Labelle, E., Grange, M.J., Elbim, C., Marquetty, C., Gougerot-Pocidalo, M.A., and Pasquier, C. Hydroxyl radical as a potential intracellular mediator of polymorphonuclear neutrophil apoptosis. Free Radic Biol Med **24,** 563, 1998.
17. Lamari, F., Braut-Boucher, F., Pongnimitprasert, N., Bernard, M., Foglietti, M.J., Derappe, C., and Aubery, M. Cell adhesion and integrin expression are modulated by oxidative stress in EA.hy 926 cells. Free Radic Res **41,** 812, 2007.
18. Barnouin, K., Dubuisson, M.L., Child, E.S., Fernandez, de Mattos, S., Glassford, J., Medema, R.H., Mann, D.J., and Lam, E.W. H_2O_2 induces a transient multi-phase cell cycle arrest in mouse fibroblasts through modulating cyclin D and p21Cip1 expression. J Biol Chem **277,** 13761, 2002.
19. Song, H., Cha, M.J., Song, B.W., Kim, I.K., Chang, W., Lim, S., Choi, E.J., Ham, O., Lee, S.Y., Chung, N., Jang, Y., and Hwang, K.C. Reactive oxygen species inhibit adhesion of mesenchymal stem cells implanted into ischemic myocardium via interference of focal adhesion complex. Stem Cells **28,** 555, 2010.
20. Gang, E.J., Bosnakovski, D., Figueiredo, C.A., Visser, J.W., and Perlingeiro, R.C. SSEA-4 identifies mesenchymal stem cells from bone marrow. Blood **109,** 1743, 2007.
21. Grimaud, E., Heymann, D., and Rédini, F. Recent advances in TGF-beta effects on chondrocyte metabolism. Potential therapeutic roles of TGF-beta in cartilage disorders. Cytokine Growth Factor Rev **13,** 241, 2002.
22. Bi, Y., Stuelten, C.H., Kilts, T., Wadhwa, S., Iozzo, R.V., Robey, P.G., Chen, X., and Young, M.F. Extracellular matrix proteoglycans control the fate of bone marrow stromal cells. J Biol Chem **280,** 30481, 2005.
23. Ferdous, Z., Wei, V.M., Iozzo, R., Höök, M., and Grande-Allen, K.J. Decorin-transforming growth factor-interaction regulates matrix organization and mechanical characteristics of three-dimensional collagen matrices. J Biol Chem **282,** 35887, 2007.
24. Asano, Y., Ihn, H., Yamane, K., Jinnin, M., and Tamaki, K. Increased expression of integrin alphavbeta5 induces the myofibroblastic differentiation of dermal fibroblasts. Am J Pathol **168,** 499, 2006.
25. Reynolds, L.E., Conti, F.J., Lucas, M., Grose, R., Robinson, S., Stone, M., Saunders, G., Dickson, C., Hynes, R.O., Lacy-Hulbert, A., and Hodivala-Dilke, K. Accelerated re-epithelialization in beta3-integrin-deficient- mice is associated with enhanced TGF-beta1 signaling. Nat Med **11,** 167, 2005.
26. Aplin, A.E., Howe, A., Alahari, S.K., and Juliano, R.L. Signal transduction and signal modulation by cell adhesion receptors: the role of integrins, cadherins, immunoglobulin-cell adhesion molecules, and selectins. Pharmacol Rev **50,** 197, 1998.
27. Goessler, U.R., Bugert, P., Bieback, K., Stern-Straeter, J., Bran, G., Sadick, H., Hbrmann, K., and Riedel, F. *In vitro* analysis of integrin expression in stem cells from bone marrow and cord blood during chondrogenic differentiation. J Cell Mol Med **13,** 1175, 2009.
28. Liaw, L., Almeida, M., Hart, C.E., Schwartz, S.M., and Giachelli, C.M. Osteopontin promotes vascular cell adhesion

and spreading and is chemotactic for smooth muscle cells *in vitro*. Circ Res **74,** 214, 1994.
29. Gladson, C.L., Dennis, C., Rotolo, T.C., Kelly, D.R., and Grammer, J.R. Vitronectin expression in differentiating neuroblastic tumors: integrin alpha v beta 5 mediates vitronectin-dependent adhesion of retinoic-acid-differentiated neuroblastoma cells. Am J Pathol **150,** 1631, 1997.
30. Shakibaei, M. Inhibition of chondrogenesis by integrin antibody *in vitro*. Exp Cell Res **240,** 95, 1998.
31. Loeser, R.F. Chondrocyte integrin expression and function. Biorheology **37,** 109, 2000.
32. Dickhut, A., Pelttari, K., Janicki, P., Wagner, W., Eckstein, V., Egermann, M., and Richter, W. Calcification or dedifferentiation: requirement to lock mesenchymal stem cells in a desired differentiation stage. J Cell Physiol **219,** 219, 2009.
33. Kurth, T.B., Dell'accio, F., Crouch, V., Augello, A., Sharpe, P.T., and De Bari, C. Functional mesenchymal stem cell niches in the adult knee joint synovium *in vivo*. Arthritis Rheum [Epub ahead of print]; DOI: 10.1002/art.30234, 2011.
34. Mochizuki, T., Muneta, T., Sakaguchi, Y., Nimura, A., Yokoyama, A., Koga, H., and Sekiya, I. Higher chondrogenic potential of fibrous synovium- and adipose synovium derived cells compared with subcutaneous fat-derived cells: distinguishing properties of mesenchymal stem cells in humans. Arthritis Rheum **54,** 843, 2006.
35. Pei, M., He, F., and Vunjak-Novakovic, G. Synovium-derived stem cell-based chondrogenesis. Differentiation **76,** 1044, 2008.
36. Sakaguchi, Y., Sekiya, I., Yagishita, K., and Muneta, T. Comparison of human stem cells derived from various mesenchymal tissues: superiority of synovium as a cell source. Arthritis Rheum **52,** 2521, 2005.
37. Segawa, Y., Muneta, T., Makino, H., Nimura, A., Mochizuki, T., Ju, Y.J., Ezura, Y., Umezawa, A., and Sekiya, I. Mesenchymal stem cells derived from synovium, meniscus, anterior cruciate ligament, and articular chondrocytes share similar gene expression profiles. J Orthop Res **27,** 435, 2009.
38. Dallari, D., Fini, M., Stagni, C., Torricelli, P., Nicoli Aldini, N., Giavaresi, G., Cenni, E., Baldini, N., Cenacchi, A., Bassi, A., Giardino, R., Fornasari, P.M., and Giunti, A. *In vivo* study on the healing of bone defects treated with bone marrow stromal cells, platelet-rich plasma, and freeze-dried bone allografts, alone and in combination. J Orthop Res **24,** 877, 2006.
39. Jones, E.A., Kinsey, S.E., English, A., Jones, R.A., Straszynski, L., Meredith, D.M., Markham, A.F., Jack, A., Emery, P., and McGonagle, D. Isolation and characterization of bone marrow multipotential mesenchymal progenitor cells. Arthritis Rheum **46,** 3349, 2002.
40. Kim, H.J., and Im, G.I. The effects of ERK1/2 inhibitor on the chondrogenesis of bone marrow- and adipose tissue-derived multipotent mesenchymal stromal cells. Tissue Eng Part A **16,** 851, 2010.
41. Pelttari, K., Winter, A., Steck, E., Goetzke, K., Hennig, T., Ochs, B.G., Aigner, T., and Richter, W. Premature induction of hypertrophy during *in vitro* chondrogenesis of human mesenchymal stem cells correlates with calcification and vascular invasion after ectopic transplantation in SCID mice. Arthritis Rheum **54,** 3254, 2006.

Address correspondence to:
Ming Pei, M.D., Ph.D.
Stem Cell and Tissue Engineering Laboratory
Division of Exercise Physiology
Department of Orthopaedics
West Virginia University
PO Box 9196
One Medical Center Drive
Morgantown, WV 26506-9196

E-mail: mpei@hsc.wvu.edu

Received: March 17, 2011
Accepted: July 8, 2011
Online Publication Date: September 21, 2011